Technical Note: The Use of RNA-interference as a Tool to Find Proteins Involved in Melanosome Formation or Transport

Eva M. Amsen[1*], Daniela Rotin[1]

1 Program in Cell Biology, The Hospital for Sick Children, and the Biochemistry Department, University of Toronto, Toronto, Ontario M5G 1X8, Canada
* Corresponding author eva.amsen@utoronto.ca

Nature Precedings : doi:10.1038/npre.2009.3419.1 : Posted 10 Jul 2009

Abstract:

Melanosomes are lysosome-related organelles that produce and transport the pigment melanin within melanocytes. Mutations in proteins required for melanosome transport and formation lead to a range of pigmentation defects, manifested at the cellular level as perinuclear clustering of melanosomes, or reduced sorting of melanosomal cargo such as tyrosinase-related protein 1 (TYRP1). A pilot screen was carried out to investigate whether a combination of cellular imaging and RNA interference could be used to identify new proteins involved in pigmentation pathways. In this study, eleven genes known to play a role in melanosome transport/formation or other pigmentation properties were knocked down in mouse melanocytes with shRNAmir constructs. The investigated genes were TYRP1, pallidin, cappuccino, dysbindin, HPS5, LYST, Myosin Va, melanophilin, RhoA, UBPY and mahogunin. In a blinded confocal imaging experiment, the only reproducible change observed in cells in which these targets were knocked down was a decrease in TYRP1 levels upon transfection with knockdown constructs against TYRP1 itself, or one of three constructs targeting HPS5 (Hermansky-Pudlak Syndrome 5). Upon analysis with high-content imaging software, only the knockdown construct against TYRP1 itself was detected. RT-PCR analysis showed that many of the shRNAmir constructs did not reduce mRNA and proteins levels enough to detect effects on melanosome properties. This was further examined for melanophilin, a protein necessary for melanosome transport. Altogether, the data show that this system is currently not sensitive enough for use in a screen for unknown regulators of melanosome transport and formation. The main obstacle appears to be incomplete reduction of target protein levels. Our observation that a ~50% reduction in mRNA level is not sufficient to elicit an effect is supported by the fact that heterozygous carriers of melanosomal transport disorders (Griscelli Syndrome, Hermansky-Pudlak Syndrome) do not display diseases phenotypes. A further reduction in protein levels, for example by viral integration of shRNA, may be required.

Introduction

Melanosomes are specialized organelles in melanocytes, responsible for the synthesis and distribution of the pigment melanin [1]. The mechanisms and proteins involved in formation and movement of melanosomes are similar to those of lysosome-related organelles in other cell types, such as synaptic vesicles in neurons, platelet dense granules in platelets, and lytic vesicles in T-cells [2-4]. In diseases such as Hermansky-Pudlak Syndrome, Chediak-Higashi Syndrome, or Griscelli Syndrome, hypopigmentation caused by a defect in either formation of movement of melanosomes is accompanied by defects in other lysosome-related organelles, causing, for example, bleeding disorders, immunological abnormalities, or neurological symptoms [5-11]. This makes melanosomes an interesting model for the study of organelle formation and transport in general.

The ultimate aim of the work described here was the development of a high-content analysis RNA interference (RNAi) screen to identify proteins that affect melanosome formation or transport. A high-content analysis system to detect changes in melanosome formation or movement was previously set up on a Cellomics HCS KineticScan Reader (Cellomics KSR) using TYRP1 as a melanosomal label (Appendix 1). To optimize this system for the identification of unknown proteins affecting melanosome properties, a set of reliable controls needed to be found first. This paper describes the testing of small hairpin RNA (shRNA) knockdown constructs that may serve as a positive control for a high-content RNAi analysis of melanosomes using Cellomics KSR. Based on a search of the literature for genes involved in various aspects of pigmentation, eleven proteins were selected for knockdown: cappuccino, pallidin, dysbindin, Hermansky Pudlak Syndrom 5 (HPS5), Myosin Va, melanophilin, lysosomal trafficking regulator (LYST), RhoA, UBPY (or ubiquitin specific peptidase 8 (USP8)), mahogunin, and tyrosinase-related protein 1 (TYRP1).

Cappuccino, pallidin, and dysbindin were originally identified as proteins that cause a severe pigmentation defect in mice when mutated[12, 13]. These three proteins are components of the biogenesis of lysosome-related organelles complex 1 (BLOC-1), required for the proper sorting of cargo (such as TYRP1) from early endosomes to lysosome-related organelles [14]. In humans, mutations in dysbindin are associated with Hermansky-Pudlak Syndrome type 7 and with an increased susceptibility to schizophrenia [15, 16]. The latter is related to the formation of synaptic vesicles, highlighting the conserved pathways between melanosomes and other lysosome-related organelles. HPS5, a protein which, when mutated, leads to Hermansky-Pudlak Syndrome type 5, is a component of the protein complex BLOC-2, which acts downstream of BLOC-1 and is also involved in the sorting of proteins to lysosome-related organelles [17, 18]. Myosin Va and melanophilin play a role in melanosome transport and are mutated in Griscelli Syndrome [5, 7, 19-22]. LYST is mutated in Chediak-Higashi syndrome, where it produces giant lysosomes and melanosomes [10, 23, 24]. Chemical inhibition of RhoA in mouse melanoma B16 cells increases dendrite extension, suggesting that its knockdown might have the same effect [25]. UBPY is a deubiquitinating enzyme required for endosomal sorting [26]. Mahogunin is an E3 ubiquitin ligase involved in regulating the melanocortin-1 receptor-mediated balance between the brown/black pigment eumelanin and the yellow/red pigment pheomelanin [27-29]. Finally, TYRP1 is involved in melanin synthesis,

and its sorting to melanosomes is regulated in part by pallidin, cappuccino, dysbindin, and HPS5 [14, 17, 30]. TYRP1 is also the label used in these experiments to detect melanosomes, and its knockdown is therefore expected to directly affect output. The known functions and predicted effects of knockdown of all proteins mentioned above are summarized in Table 1.

In this study, the effect of knockdown of all target proteins was investigated in a blinded experiment using confocal microscopy. Knockdown of TYRP1 and HPS5 both showed a reproducible decrease in TYRP1 levels, but only knockdown of TYRP1 itself was detected using the Cellomics KSR. Limited knockdown and residual protein expression appear to be the major cause for the lack of effect of any of the other selected targets.

Methods

Cell Culture and Constructs

Melan-a cells were obtained from the Wellcome Trust Functional Genomics Cell Bank and cultured at 37°C and 10% CO_2 in RPMI-1640 with L-glutamine (Invitrogen, cat. 11875) supplemented with 10% FBS, 100U/ml penicillin, 100 μg/ml streptomycin, 7.5 μg/ml phenol red, 0.1 mM 2-mercaptoethanol, 2.7 mM HCl, and 200 nM PMA (added prior to use).

Mouse genomic pGIPZ- shRNAmir vectors from the Hannon-Elledge library were purchased from Open Biosystems. These vectors express TurboGFP and transcribe an shRNAmir hairpin, both using a CMV promotor [31]. pGIPZ constructs used are listed in Table 4-2.

Cells for confocal analysis were transfected using Lipofectamine 2000 (Invitrogen) according to the manufacturer's protocol, using 1μg DNA and 3 μl lipofectamine 2000 per well in a 4-well chamber slide, seeded with 100,000 cells the previous day. Cells for Cellomics analysis were transfected as follows: Melan-a cells were transfected using Lipofectamine 2000 (Invitrogen) according to the manufacturer's protocol, using 0.25 μg DNA per well and 0.6 μl lipofectamine 2000 per well in a 96-well plate.

Immunostaining

For confocal analysis, cells were grown in 4-well polystyrene vessel glass slides (BD Falcon). At 48 or 72 hours after transfection with pGIPZ vectors, cells were fixed and stained for immunofluorescence. All steps were carried out at room temperature and without shaking to avoid cells detaching from the slide, and in the dark to avoid photobleaching. Samples were first stained for 5 minutes with Alexa-647 labeled Concanavalin A (Molecular Probes) to label the plasma membrane. The cells were then washed in PBS and fixed in 4% paraformaldehyde (PFA) in PBS for 20 minutes and permeabilized with a buffer of 0.1% Triton-X 100 and 1% BSA in PBS. Cells were blocked for 1 hour in 5% donkey serum (Jackson ImmunoResearch Laboratories). Samples were incubated for 1 hour with a mouse monoclonal antibody against TYRP1 (AbCam) at 1:1000 dilution and a rabbit polyclonal antibody against TurboGFP (Evrogen) at 1:10,000 dilution in 1%BSA in PBS. After this, cells were washed three

times with 1% BSA in PBS, and incubated 45 minutes with Cy3-labeled donkey-anti-mouse $F(ab')_2$ (Jackson ImmunoResearch Laboratories) at 1:1000 and FITC-labeled donkey-anti-rabbit (Jackson ImmunoResearch Laboratories) secondary antibody in 1% BSA in PBS. After washing with PBS, slides were mounted using DAKO® Fluorescent mounting medium.

To detect melanophilin knockdown by immunofluoresccnce, the same protocol was used, but with a goat polyclonal antibody against melanophilin (AbCam, 1:1000 dilution) instead of TYRP1 antibody, and secondary antibody 1:1000 donkey-anti-goat Cy3 (Jackson ImmunoResearch Laboratories) instead of donkey-anti-mouse $F(ab')_2$

For Cellomics KSR analysis, cells were grown in 96-well plates (Corning), transfected as described, and fixed at the indicated times in 4% PFA in PBS. After fixation, permeabilization and immunostaining were carried out as described above until the final PBS wash step. Then cells were incubated for 5 minutes with DAPI nucleic acid stain (Molecular Probes), washed again, and kept in PBS (100 μl per well).

Confocal Analysis

Confocal analysis was carried out on a Zeiss Axiovert 200 inverted fluorescence microscope with 63X 1.2 water immersion C-Apochromat objective and analyzed with LSM510 software. To quantify levels of TYRP1 per cell, Volocity software was used to measure the total intensity of the Cy3 signal in all GFP-expressing cells, as well as the total intensity of the Cy3 signal in a similar number of cells that did not express GFP in the same fields, to account for variations in signal intensity between samples. Results were analyzed and presented using GraphPad, where error bars show the Standard Error of the Mean (S.E.M.) and unpaired T-test analysis was used to determine statistical significance between transfected and untransfected cells. The same protocol was followed to quantify melanophilin knockdown by immunofluorescence.

Cellomics KSR analysis

Plates were scanned on a Cellomics KineticScan® HCS Reader with 10x Plan-Neofluar objective. Images were acquired in 20 fields per well and in the following channels: DAPI was detected in XF93 Hoechst (0.040 second exposure), Cy3 in XF93 TRITC (0.500 second exposure) and FITC-labeled TurboGFP in the XF93 FITC channel (0.500 second exposure). Each well was measured once (kinetic scan set to “single time point”).

To determine TYRP1 levels, the SpotDetector BioApplication was used with the settings as shown in Appendix 1. Two protocol settings were used to measure spots: one measured transfected cells (SpotAvgIntenCh3 min = 25) and the other measured untransfected cells (SpotAvgIntenCh3 max = 24.999).

RNA isolation and First Strand Synthesis

To analyse mRNA levels after knockdown, cells were transfected with pGIPZ constructs and GFP-expressing cells were collected on a BD Aria-RITT sorter by fluorescence-activated cell sorting (FACS) after 72 hours. Collected cells were immediately lysed in 800 μl TRIZOL Reagent (Invitrogen) according to the manufacturer’s protocol. After phase separation with chloroform, 0.5 μl glycogen was added as a carrier to the aqueous

phase. Final RNA pellet was taken up in 12 μl DEPC-treated water. After determining RNA concentration in the sample, 8 μl was converted to cDNA using the SuperScript III First-Strand Synthesis System for RT-PCR (real-time PCR) (Invitrogen) according to the manufacturer's protocol.

RT-PCR analysis

After first-strand synthesis, cDNA levels of genes of interest were determined using quantitative PCR with Platinum SYBR Green qPCR SuperMix-UDG (Invitrogen), using 12.5 μl SYBR Green, 1 ml each of forward and reverse primer (10 μM), 8.5 μl H2O and 2 μl cDNA template. Primers are listed in table 4.3. All primers were designed to cross intron-exon boundaries, except primers for Cappuccino, which only has one exon. (For Cappuccino, RNA samples were treated with DNase to ensure removal of genomic DNA.) Samples were run for forty cycles (30 seconds 95ºC, 30 seconds 54 or 55ºC (depending on primers), 30 seconds 72ºC) on a Bio-Rad Chromo 4 Real-Time PCR detector and analyzed with Opticon Monitor and Genex (Bio-Rad) software. Expression levels were normalized to levels in cells transfected with the non-silencing control.

Results

Blinded confocal experiment to test pilot set of shRNA constructs

In order to find a suitable control for high content analysis of proteins involved in melanosome formation or sorting, a blinded confocal analysis was carried out to find proteins for which knockdown results in a clearly detectable change in TYRP1 staining levels or location.

Twenty-three pGIPZ constructs, against eleven target genes, were used to transfect melan-a cells in a blinded experiment, for which samples were relabeled and reordered. Cells were grown in four-well chamber slides. On every slide one well was transfected with a non-silencing control and three wells were transfected with blinded knockdown vectors. After fixing and staining, twenty confocal images were taken of every well. During this process two things were immediately obvious: First, there was a lot of variation in phenotype even among untransfected cells or non-silencing controls, and second, many transfected cells did not look any different from untransfected cells. The only obvious phenotype seen in some samples was a reduction in TYRP1 levels as visualized by a Cy3-tagged antibody. Figure 1 shows this reduction at 72 hour knockdown for two samples, which, after unblinding, were identified as samples in which either TYRP1 (top) or HPS5 (bottom) was knocked down.

To quantify this observation, TYRP1 levels in transfected cells (identified by TurboGFP expression) were compared to TYRP1 levels in untransfected cells in the same well. TYRP1 levels per cell were measured using Volocity software and analyzed in GraphPad, where T-test analysis was used to determine whether the difference in TYRP1 levels between transfected and untransfected cells was statistically significant. The P-values obtained from this analysis are shown in Table 4, and graphs are shown in Figure 2 (48 hour knockdown) and Figure 3 (72 hour knockdown).

At 72 hour knockdown, more samples show a higher statistically significant difference in TYRP1 levels between transfected and untransfected cells than at 48 hour knockdown. However, a statistically significant difference between transfected and untransfected cells does not necessarily correlate with a biologically significant difference. This is clear from the data collected from non-silencing controls: After both 48 hour and 72 hour transfections, two out of eight non-silencing controls show a statistically significant ($P<0.05$) reduction in TYRP1 levels in transfected cells compared to untransfected cells in the same wells. This suggests that there is a strong possibility that about a quarter of all "hits" for which $P<0.05$ are a false positive. To indicate this, the samples are ranked by reproducibility and P value in Table 4. Samples where a significant change in TYRP1 levels was observed at both 48 and 72 hour knockdown are at the top, followed by samples that were only significant at 72 hour knockdown with $P<0.01$ or $P<0.001$. Under the horizontal line are all samples that only showed up as statistically significant for one time point with $P<0.05$ – in other words, all the samples that were no more significant than 25% of the negative controls.

To investigate reproducibility, six of the top hits were analyzed again using confocal microscopy on cells fixed 72 hours after transfection. In this experiment, only two samples showed the same effect as before: knockdown of TYRP1 with construct v2LMM_12467 and knockdown of HPS5 with construct v2LMM_224489 (Table 4).

Cellomics KSR High-Content Analysis of selected shRNA constructs

Next, we investigated whether Cellomics KSR analysis would be able to pick up the same samples that show a reproducible reduction in TYRP1 on confocal analysis. The Cellomics KSR is a high-content imaging platform, which calculates several output values using specific image analysis algorithms called BioApplications, for which parameters can be adjusted by the user. Detection settings for melanosomes were previously optimized using this system with the Spot Detector BioApplication. Parameters for optimal detection of melanosomes are listed in Appendix 1.

The Spot Detector BioApplication defines spots as localized regions of increased TYRP1 intensity in a predefined area around the nucleus of every cell. Because TYRP1 is specifically sorted to melanosomes, spots are roughly equivalent to melanosomes in this model. The algorithm returns several output values after image analysis, such as the number or size of spots per cell, or the signal intensity per spot or per cell.

Melan-a cells grown in a 96-well plate were transfected with the constructs giving the strongest effects in the confocal experiment (v2LMM_12467 against TYRP1, v2LMM_76067 against dysbindin, v2LMM196168 and v2LMM_224489 against HPS5, v2LMM_7485 against Myosin Va, and v2LMM_37945 against UBPY) or with a non-silencing control. The plate was fixed and stained after 72 hours and analyzed on Cellomics KSR with the Spot Detector BioApplication. Because the phenotype observed in confocal analysis was a reduction in TYRP1 levels, the Spot Detector BioApplication output value SpotTotalIntenPerObjectCh2 (reporting the total intensity of the Cy3-labeled TYRP1 per cell) was expected to most closely resemble results obtained on confocal analysis.

The Spot Detector BioApplication was run twice: once reporting output values for TYRP1-labeled spots in transfected cells and the second time carrying out the same measurements on untransfected cells. Transfected cells were detected on the Cellomics KSR in the FITC channel. The pGIPZ vector expressed TurboGFP, which is itself fluorescent, but bleaches upon fixing cells with PFA. The TurboGFP signal was enhanced by labeling cells with an antibody against TurboGFP and a secondary FITC-labeled antibody. To emulate the comparison of transfected and untransfected cells per well, which was expressed using P-values in confocal analysis, the SpotTotalIntenPerObjectCh2 output value for transfected cells was normalized over the value obtained from untransfected cells in the same well. For wells where the TYRP1 intensity is very similar between transfected and untransfected cells, this value approaches 1. For wells where the difference between transfected and untransfected cells is large (corresponding to a low P-value in the confocal experiment) the normalized TYRP1 intensity on Cellomics analysis is low. Other output values, such as the number or size of the spots, were calculated by Cellomics KSR but showed no difference between any of the samples and the negative controls, so only the TYRP1 intensity is reported here.

Figure 4 shows the normalized result of a Cellomics scan for the top hits of the confocal analysis, reported in grid fashion corresponding to the order of the samples on the plate. To better visualize the data, colours were assigned to normalized levels on the red-green scale, where red represents the lowest normalized values and green the values closest to 1. It is obvious from this figure that only knockdown of TYRP1 itself reduced TYRP1 enough to be detected by Cellomics KSR with Spot Detector BioApplication. In this figure, all six transfections with pGIPZ against TYRP1 correspond to the six wells with the lowest TYRP1 levels in transfected cells. In a repeat experiment, five out of six TYRP1 knockdown transfections had the lowest reported TYRP1 values of the plate (not shown). None of the other transfections are detected as hits in this analysis. V2LMM_224489, the knockdown construct against HPS5 that was a reproducible hit in the confocal microscopy experiment does not appear to show any further TYRP1 reduction than non-silencing controls.

Validation of Knockdown

The above results indicate that, other than TYRP1 itself, none of the knockdown constructs reduce TYRP1 levels enough to be detectable by Cellomics KSR analysis. Nevertheless, these target genes were selected based on their predicted effects on melanosome properties or other aspects of pigmentation. According to the literature, reduction of TYRP1 levels was expected for knockdown of BLOC-1 or BLOC-2 components (pallidin, dysbindin, cappuccino, HPS5) and altered distribution of melanosomes was expected upon knockdown of Myosin Va or melanophilin.

To investigate what caused the absense of expected phenotypic changes, knockdown levels were determined using quantitative real time PCR (RT-PCR) on cDNA prepared from FACS sorted cells transfected with pGIPZ constructs. The residual mRNA levels in every RT-PCR experiment were normalized to mRNA levels for the protein of interest in cells transfected with a non-silencing control plasmid. Figure 5 shows the results of these experiments. Every sample was measured at least in triplicate (most samples in

quadruplicate) and some experiments were repeated in their entirety to confirm that the RT-PCR results were indeed reproducible.

The results indicate that of the investigated proteins, TYRP1 is most effectively knocked down by its corresponding shRNA construct, reducing mRNA levels to approximately 5-15% of the levels in non-silencing control (results from two separate experiments each measured in quadruplicate). Since TYRP1 was used as melanosomal label in all confocal and microscopy experiments, the approximate reduction in protein level for this knockdown construct could be determined: Cellomics analysis of spot intensity shows that TYRP1 protein levels were reduced to ~50-60% compared to both TYRP1 levels in untransfected cells in the same well, and to TYRP1 levels in cells transfected with a non-silencing control in the same plate.

While TYRP1 mRNA levels were reduced by about 90%, knockdown of other proteins, such as mahogunin or LYST, was minimal, even at the mRNA level. This may explain why cells transfected with these knockdown constructs did not differ from negative controls. Other constructs, such as those targeting cappuccino, show a reduction of about 50% at the mRNA level, but no effect on TYRP1 levels in confocal analysis.

Melanophilin Knockdown

Many of the proteins targeted in these experiments had been studied previously by others, using cells from mutant mice or from human patients with pigmentation disorders, but not using knockdown in cultured melanocytes. Only knockdown of melanophilin in melan-a cells was previously reported [21]. Kuroda and Fukuda showed an expected perinuclear distribution in cells in which melanophilin levels were reduced, but we did not observe a similar distribution pattern in cells transfected with any of the three pGIPZ constructs against melanophilin. RT-PCR results show that none of these constructs strongly reduce melanophilin levels. Only v2LMM_73840 reduces mRNA levels by about 50%.

In these studies, knockdown efficiency was determined by RT-PCR rather than a direct measurement of protein levels for several reasons: melan-a cells did not yield enough cells after FACS sorting to carry out western blot analysis, FACS-sorted cells did not survive reseeding to increase cell number, and for many of the proteins investigated no antibodies were available. There is, however, a commercially available antibody against melanophilin. Using this antibody, residual protein levels were measured upon melanophilin knockdown using confocal analysis and Volocity software, as was done for TYRP1 levels. After Volocity analysis of melanophilin levels, it became clear that even though there is a slight reduction of melanophilin at the mRNA level, the protein levels are not markedly reduced (Figure 6). However, there is a large variation in melanophilin levels between individual cells, as shown by the distribution of intensities in Figure 6. Figure 7 shows the confocal images of a cell with very little melanophilin levels. The bright field image of this particular cell does appear to show a perinuclear localization of melanosomes, and in a repeat experiment, a few other cells with very low melanophilin levels also showed perinuclear localization. This highlights the variation in phenotype within a sample, and furthermore suggests that protein levels need to be very low to detect any effect of melanophilin reduction.

Discussion

Eleven genes that are either known to be directly involved in melanosome development or transport, or likely to affect pigmentation or organelle formation, were knocked down in melan-a cells using pGIPZ shRNAmir constructs from the Hannon-Elledge shRNAmir library. Of the eleven proteins knocked down in these experiments, only TYRP1 knockdown (using v2LMM_12467) caused phenotypic changes that were repeatedly detected by both confocal and Cellomics analysis (Figures 2 and 4). Not only is TYRP1 the protein that showed the largest decrease in mRNA levels upon knockdown (Figure 5), but its knockdown is also the direct output value measured in these systems. Knockdown of all other proteins is measured indirectly in terms of their effect on TYRP1 levels. The Cellomics KSR was not able to accurately detect the indirect effect of HPS5 knockdown by v2LMM_224489 on TYRP1 levels, even though this is detected in confocal analysis (Figures 2 and 4). The observed reduction of TYRP1 levels in response to HPS5 knockdown by v2LMM_224489 is, however, in line with observations by others: In melanocytes of HPS5 patients, TYRP1 levels are significantly reduced [17].

HPS5 is a component of the BLOC-2 complex, which is involved in the sorting of TYRP1 to melanosomes [18]. Based on this, an effect of knockdown of dysbindin, pallidin, and cappuccino was also expected. These proteins are components of the BLOC-1 complex, which is also required for TYRP1 sorting and acts upstream of BLOC-2. Mice lacking any of the BLOC-1 proteins are hypopigmented - almost white [13]. However, none of the knockdown constructs against these proteins caused a reproducible effect on TYRP1 levels (Figures 2 - 4 and table 4). RT-PCR showed negligible knockdown of dysbindin (Figure 5). Cappuccino and pallidin knockdown constructs reduce mRNA levels to about 50-70% of control levels, but this appears to have no effect on TYRP1 levels, even though a relation between pallidin and TYRP1 levels has been shown by others [14]. However, in work by Setty *et al.*, mice with mutant inactive pallidin were studied, and in our experiments at least 50% of residual pallidin is still present (possibly more at the protein level).

It should be noted that Hermansky-Pudlak Syndrome and Griscelli Syndrome are both recessive disorders [5-8]. Carriers, with only one mutated gene (heterozygotes), do not show the disease phenotype. This supports out observation that an approximate 50% reduction in mRNA levels does not lead to a phenotypic change. In light of this, it appears that many of the genes investigated here are not sufficiently knocked down to cause downstream effects. The Hannon-Elledge library reportedly achieved 60% reduction of RNA levels or more for about 80% of the constructs in a test set [31]. In this work, a similar reduction is observed in only 6 of 23 tested constructs (Figure 5). It is possible that knockdown is cell-line specific, or that this particular set of shRNAmir constructs shows below average knockdown efficiency.

In addition, depending on the half-life of the protein, a reduction in mRNA levels may have little effect on protein levels. This is illustrated by the observed knockdown of melanophilin: even though v2LMM_73840 appeared to reduce melanophilin levels to approximately 50% of control, no overall reduction was detected at the protein level (Figures 5C and 6). Only in cells with extremely low melanophilin protein levels (intensity ~20% of the mean melanophilin intensity) was perinuclear localization visible (Figure 7). A recent study also showed that Myosin Va, which is part of the same

transport complex, requires prolonged knockdown in order to see an effect on melanosome location [32].

In conclusion, investigation of knockdown of a small set of proteins suggests that transient transfection of pGIPZ RNAi constructs is not sufficient to identify proteins involved in melanosome formation or transport using high-content RNAi screening: Many constructs show only limited knockdown at the mRNA level, residual protein (even after mRNA removal) may still elicit an effect, and the melanosomal system appears to be particularly robust to changes in protein levels, requiring near depletion of proteins to elicit an effect. These problems can potentially be overcome in part by lentiviral infection of the knockdown construct, which allows the pGIPZ hairpin to integrate into the genome and reduce protein levels over a longer period of time.

Acknowledgements:

Cellomics KSR analysis was carried out at the Signalling Identification Network (SIDNET) of The Hospital for Sick Children. This work was supported by the National Cancer Institute of Canada (NCIC) with funds from the Canadian Cancer Society. E.A. was supported in part through a studentship by the Ontario Student Opportunity Trust Fund-Hospital for Sick Children Foundation Student Scholarship Program

References

1. Seiji, M., Shimao, K., Birbeck, M. S. & Fitzpatrick, T. B. Subcellular localization of melanin biosynthesis. *Ann. N. Y. Acad. Sci.* **100**, 497-533 (1963).

2. Barral, D. C. & Seabra, M. C. The melanosome as a model to study organelle motility in mammals. *Pigment Cell Res.* **17**, 111-118 (2004).

3. Stinchcombe, J., Bossi, G. & Griffiths, G. M. Linking albinism and immunity: the secrets of secretory lysosomes. *Science* **305**, 55-59 (2004).

4. Orlow, S. J. Melanosomes are specialized members of the lysosomal lineage of organelles. *J. Invest. Dermatol.* **105**, 3-7 (1995).

5. Pastural, E. *et al*. Griscelli disease maps to chromosome 15q21 and is associated with mutations in the myosin-Va gene. *Nat. Genet.* **16**, 289-292 (1997).

6. Ménasché, G. *et al*. Mutations in RAB27A cause Griscelli syndrome associated with haemophagocytic syndrome. *Nat. Genet.* **25**, 173-176 (2000).

7. Ménasché, G. *et al*. Griscelli syndrome restricted to hypopigmentation results from a melanophilin defect (GS3) or a MYO5A F-exon deletion (GS1). *J. Clin. Invest.* **112**, 450-456 (2003).

8. Wei, M. L. Hermansky-Pudlak syndrome: a disease of protein trafficking and organelle function. *Pigment Cell Res.* **19**, 19-42 (2006).

9. Hermansky, F. & Pudlak, P. Albinism associated with hemorrhagic diathesis and unusual pigmented reticular cells in the bone marrow: report of two cases with histochemical studies. *Blood* **14**, 162-169 (1959).

10. Burkhardt, J. K., Wiebel, F. A., Hester, S. & Argon, Y. The giant organelles in beige and Chediak-Higashi fibroblasts are derived from late endosomes and mature lysosomes. *J. Exp. Med.* **178**, 1845-1856 (1993).

11. Page, A. R., Berendes, H., Warner, J. & Good, R. A. The Chediak-Higashi syndrome. *Blood* **20**, 330-343 (1962).

12. Nguyen, T. *et al*. Melanosome morphologies in murine models of Hermansky-Pudlak syndrome reflect blocks in organelle development. *J. Invest. Dermatol.* **119**, 1156-1164 (2002).

13. Li, W. *et al*. Murine Hermansky-Pudlak syndrome genes: regulators of lysosome-related organelles. *Bioessays* **26**, 616-628 (2004).

14. Setty, S. R. *et al*. BLOC-1 is required for cargo-specific sorting from vacuolar early endosomes toward lysosome-related organelles. *Mol. Biol. Cell* **18**, 768-780 (2007).

15. Chen, X. W. *et al*. DTNBP1, a schizophrenia susceptibility gene, affects kinetics of transmitter release. *J. Cell Biol.* **181**, 791-801 (2008).

16. Li, W. *et al*. Hermansky-Pudlak syndrome type 7 (HPS-7) results from mutant dysbindin, a member of the biogenesis of lysosome-related organelles complex 1 (BLOC-1). *Nat. Genet.* **35**, 84-89 (2003).

17. Helip-Wooley, A. *et al*. Improper trafficking of melanocyte-specific proteins in Hermansky-Pudlak syndrome type-5. *J. Invest. Dermatol.* **127**, 1471-1478 (2007).

18. Di Pietro, S. M. *et al*. BLOC-1 interacts with BLOC-2 and the AP-3 complex to facilitate protein trafficking on endosomes. *Mol. Biol. Cell* **17**, 4027-4038 (2006).

19. Wei, Q., Wu, X. & Hammer, J. A.,3rd. The predominant defect in dilute melanocytes is in melanosome distribution and not cell shape, supporting a role for myosin V in melanosome transport. *J. Muscle Res. Cell. Motil.* **18**, 517-527 (1997).

20. Fukuda, M., Kuroda, T. S. & Mikoshiba, K. Slac2-a/melanophilin, the missing link between Rab27 and myosin Va: implications of a tripartite protein complex for melanosome transport. *J. Biol. Chem.* **277**, 12432-12436 (2002).

21. Kuroda, T. S. & Fukuda, M. Rab27A-binding protein Slp2-a is required for peripheral melanosome distribution and elongated cell shape in melanocytes. *Nat. Cell Biol.* **6**, 1195-1203 (2004).

22. Matesic, L. E. *et al.* Mutations in Mlph, encoding a member of the Rab effector family, cause the melanosome transport defects observed in leaden mice. *Proc. Natl. Acad. Sci. U. S. A.* **98**, 10238-10243 (2001).

23. Tchernev, V. T. *et al.* The Chediak-Higashi protein interacts with SNARE complex and signal transduction proteins. *Mol. Med.* **8**, 56-64 (2002).

24. Fukai, K. *et al*. Homozygosity mapping of the gene for Chediak-Higashi syndrome to chromosome 1q42-q44 in a segment of conserved synteny that includes the mouse beige locus (bg). *Am. J. Hum. Genet.* **59**, 620-624 (1996).

25. Busca, R. *et al.* Inhibition of Rho is required for cAMP-induced melanoma cell differentiation. *Mol. Biol. Cell* **9**, 1367-1378 (1998).

26. Mizuno, E., Kobayashi, K., Yamamoto, A., Kitamura, N. & Komada, M. A deubiquitinating enzyme UBPY regulates the level of protein ubiquitination on endosomes. *Traffic* **7**, 1017-1031 (2006).

27. Bagher, P., Jiao, J., Owen Smith, C., Cota, C. D. & Gunn, T. M. Characterization of Mahogunin Ring Finger-1 expression in mice. *Pigment Cell Res.* **19**, 635-643 (2006).

28. Kim, B. Y., Olzmann, J. A., Barsh, G. S., Chin, L. S. & Li, L. Spongiform neurodegeneration-associated E3 ligase Mahogunin ubiquitylates TSG101 and regulates endosomal trafficking. *Mol. Biol. Cell* **18**, 1129-1142 (2007).

29. Phan, L. K., Chung, W. K. & Leibel, R. L. The mahoganoid mutation (Mgrn1md) improves insulin sensitivity in mice with mutations in the melanocortin signaling pathway independently of effects on adiposity. *Am. J. Physiol. Endocrinol. Metab.* **291**, E611-20 (2006).

30. Ito, S. & Wakamatsu, K. Chemistry of mixed melanogenesis--pivotal roles of dopaquinone. *Photochem. Photobiol.* **84**, 582-592 (2008).

31. Silva, J. M. *et al*. Second-generation shRNA libraries covering the mouse and human genomes. *Nat. Genet.* **37**, 1281-1288 (2005).

32. Van Gele, M., Geusens, B., Schmitt, A. M., Aguilar, L. & Lambert, J. Knockdown of Myosin Va Isoforms by RNAi as a Tool to Block Melanosome Transport in Primary Human Melanocytes. *J. Invest. Dermatol.* (2008).

Table 1

Protein	Function
TYRP1	Required for synthesis of eumelanin. Sorted to late stage melanosomes.
Cappuccino	Component of BLOC-1
Pallidin	Component of BLOC-1. Mice with a mutation in pallidin have almost no mature melanosomes, and TYRP1 sorting is impaired
Dysbindin	Component of BLOC-1. Mice with a mutation in dysbindin have almost no mature melanosomes. In humans, dysbindin mutations are associated with Hermansky-Pudlak Syndrome type 7 and with schizophrenia
HPS5	Component of BLOC-2. Mutated in Hermansky-Pudlak Syndrome type 5 patients, and reduces number of mature melanosomes and TYRP1 levels in these patients
LYST	Mutated in Chediak-Higashi Syndrome. Mutation leads to formation of giant lysosomes and melanosomes.
Myosin Va	Mutated in Griscelli Syndrome Type 1. Necessary for transport of melanosomes.
Melanophilin	Mutated in Griscelli Syndrome Type 3. Necessary for transport of melanosomes. Knockdown in melan-a cells causes perinuclear localization of melanosomes.
UBPY (USP8)	Deubiquitinating enzyme, necessary for proper sorting to endosomes. Knockdown in HeLa cells affects shape of endosomes and MVBs. Mouse mutant is embryonic lethal.
Mahogunin	an E3 ubiquitin ligase required for endosome to lysosome trafficking and for pigment type switching between eumelanin and pheomelanin.
RhoA	Chemical inhibition in B16 cells induces dendrite outgrowth

Table 1: Proteins selected for knockdown in experiments searching for a positive control for Cellomics KSR analysis. These targets have been linked to melanin synthesis (TYRP1, Mahogunin), development of melanosomes or other lysosome-related organelles (cappuccino, pallidin, dysbindin, HPS5, LYST, UBPY), transport of melanosomes (Myosin Va, melanophilin) or dendrite extension (RhoA). (see text for references)

Table 2

Gene name	GenBank ID (mouse)	Open Biosystems Construct ID
TYRP1	NM_031202	v2LMM_12467
Cappuccino	NM_133724	v2LMM_21767 v2LMM_250967
Pallidin	NM_019788	v2LMM_24372 v2LMM_28461 v2LMM_36292
Dysbindin	NM_025772	v2LMM_76067
HPS5	NM_001005248	v2LMM_196168 v2LMM_92618 v2LMM_224489
LYST	NM_010748	v2LMM_4222 v2LMM_11529 v2LMM_10733
Myosin Va	NM_010864	v2LMM_4868 v2LMM_7485 v2LMM_17673
Melanophilin	AF384098	v2LMM_73840 v2LMM_70729 v2LMM_62443
UBPY	NM_019729	v2LMM_37945
Mahogunin	NM_029657	v2LMM_66590 v2LMM_75408
RhoA	NM_016802	v2LMM_50451
Non-silencing control		RHS4346*

Table 2: pGIPZ constructs transcribing hairpins from the Hannon-Ellegde shRNAmir library were obtained from OpenBiosystems. Every available shRNAmir hairpin against each gene is listed. GenBank IDs refer to the mouse genome.

Table 3

	RT-PCR primer pairs		
Gene	**Forward primer**	**Reverse primer**	**PCR product size (bp)**
TYRP1	ACACTTTGTAACAGCACTGAG	ATCATTGGGAGACAAATGGGT	290
Dysbindin	GAAGCCTTCAAAGCTGAACTC	ACATCACAATGTTGTCCTCTC	300
Pallidin	CTGCTGTCCCACTACTTACC	CATCTCCTTCCTTATAGTCACCAG	200
Cappuccino	CAGGATGGAGGAGCAGGTC	CTCGGTCCGAAACAGGACT	163
HPS5	ACACCAGTTCAAGAAGCTCC	GCTACATCCTGAATATCCTTGAC	230
Melanophilin	ATGTAGCCCTTTACCCTCTG	CTCCAAGATCTGAGTCTCAGG	243
Myosin Va	GGAGAGGAAGTTAGTAGAAGAG	TTAGGCACATTCAGCATCAG	152
LYST	CCATCATAAGCCTGACATTCTC	GACACTCCTTCTCTTCATCC	162
RhoA	CTTCAATCCAGAAGAAACTGGTG	GCGGTCATAATCTTCTTGTCC	204
UBPY	TATTTCAACCGAAACTGCTACC	CCGATTGTCAGCCTTATTCAG	260
Mahogunin	ATGATGAGCTGAACTTTGACC	TTGTTCTTGTTCTCGATGCC	228
Actin	GATGACCCAGATCATGTTTGAG	CTTCTCTTTGATGTCACGCAC	291

Table 3: Primers used for RT-PCR. To avoid amplifying residual genomic DNA all primers were designed (with PerlPrimer) to cross intron-exon boundaries with the exception of those against the single-exon gene Cappuccino

Table 4

pGIPZ ID	gene	Knockdown 48 hr	Knockdown 72 hr	Retested 72hr
v2LMM_12467	TYRP1	**	**	***
v2LMM_76067	Dysbindin	*	***	
v2LMM_196168	HPS5	*	*	
v2LMM_224489	HPS5		***	***
v2LMM_7485	Myosin Va		***	
v2LMM_37945	UBPY		**	
v2LMM_75408	Mahogunin		*	
v2LMM_36292	Pallidin		*	
v2LMM_50451	RhoA		*	
v2LMM_73840	Melanophilin		*	
v2LMM_4222	LYST	*		
v2LMM_4868	Myosin Va	*		
v2LMM_21767	Cappuccino	*		
v2LMM_17673	Myosin Va	*		
v2LMM_24372	Pallidin			
v2LMM_28461	Pallidin			
v2LMM_92618	HPS5			
v2LMM_70729	Melanophilin			
v2LMM_11529	LYST			
v2LMM_10733	LYST			
v2LMM_62443	Melanophilin			
v2LMM_66590	Mahogunin			
v2LMM_250967	Cappuccino			

Table 4: Results from confocal experiments

To quantify results from the confocal experiments (see Figures 2 and 3), TYRP1 levels were measured using Volocity software for both transfected and untransfected cells in each sample, and a ranking order was based on P-values for unpaired T-test between measurements from transfected and untransfected cells. Samples that showed a statistically significant ($P<0.05$) difference between transfected and untransfected cells at both 48 hour and 72 hour knockdown were ranked highest, followed by those which only showed a significant difference at 72 hour knockdown, followed by samples only significant at 48 hour knockdown or not at all.

At both time points (48 and 72 hour knockdown), two out of eight negative controls samples (transfected with non-silencing pGIPZ plasmid) showed a difference in TYRP1 levels between transfected and untransfected cells with $P<0.05$ (see Figures 2 and 3). Therefore, any samples that only showed up once with $P<0.05$ were considered no more significant than negative controls. This is indicated by a horizontal line in table 4.

The top samples (above the horizontal line) were retested at 72 hour knockdown, and only v2LMM_12467 and v2LMM_224489 showed a reproducible effect on TYRP1 levels.

Data were collected in blinded experiments and later annotated with the corresponding pGIPZ ID numbers.

Figure 1

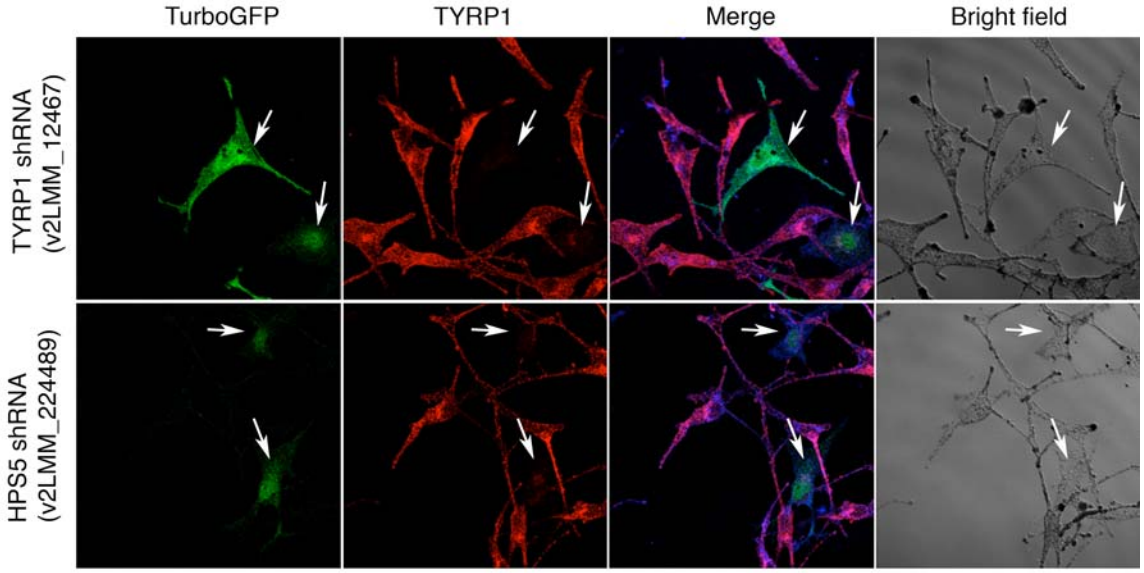

Figure 1: Reduction of TYRP1 levels

After 72 hour transfection, some cells transfected with the pGIPZ constructs v2LMM_12467 (against TYRP1, top) or v2LMM_224489 (against HPS5, bottom) showed a decrease in TYRP1 levels (arrows in second column).

Figure 2

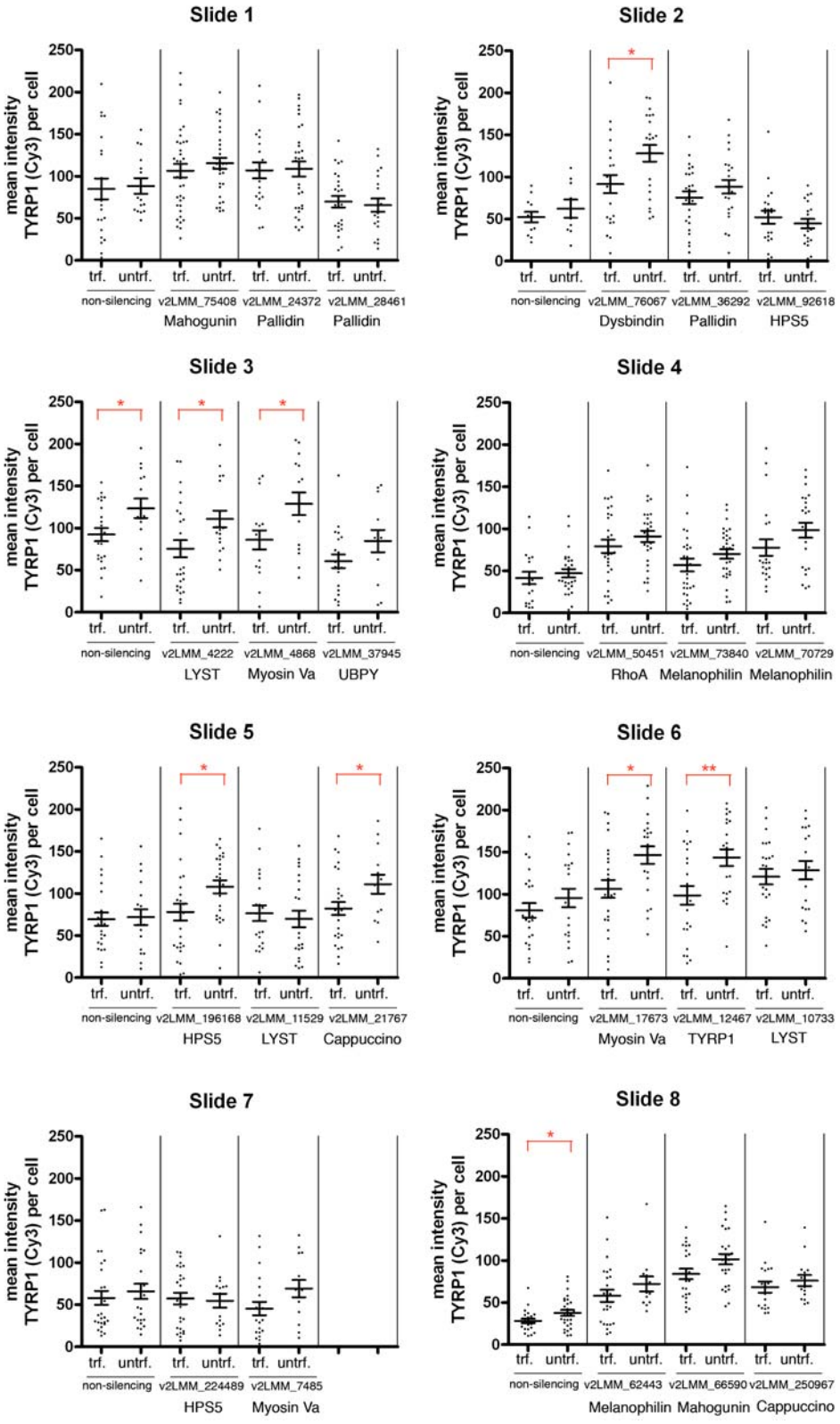

Figure 2: Quantified TYRP1 levels per cell after 48 hour transfection with pGIPZ constructs.

For each sample of melan-a cells grown in 4-well chamber slides, TYRP1 levels per cell were determined using Volocity software for both transfected and untransfected cells, to account for variations in TYRP1 intensity between wells or slides. The differences between values for transfected and untransfected cells per sample were evaluated using an unpaired T-test, and asterisks indicate statistical significance: *=$P<0.05$, **=$P<0.01$, ***=$P<0.001$. P-values for these samples are ranked in Table 4. Data were collected in a blinded experiment and later annotated with the correct pGIPZ ID. Error bars indicate standard error of the mean.

Figure 3

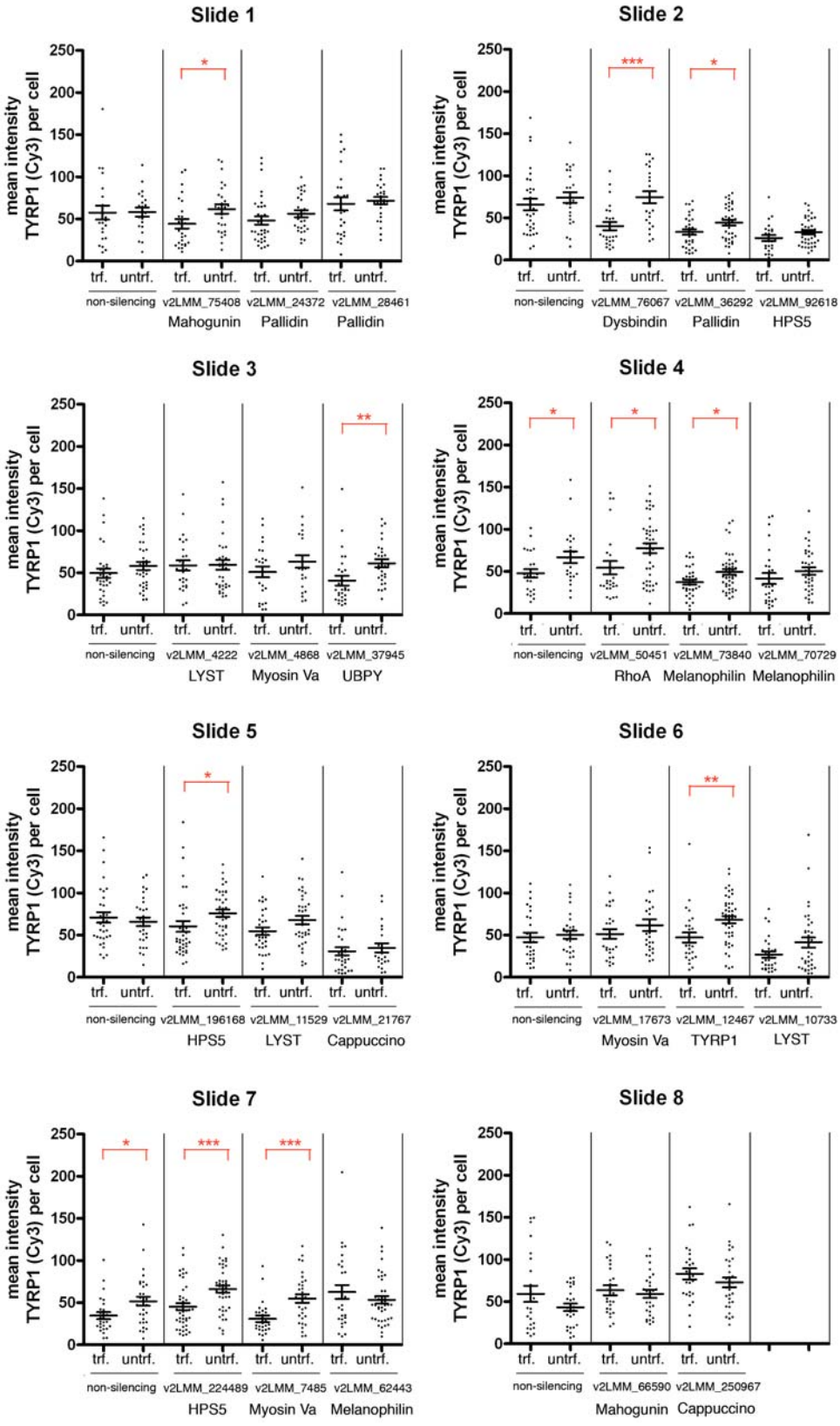

Figure 3: Quantified TYRP1 levels per cell after 72 hour transfection with pGIPZ constructs.

For each sample of melan-a cells grown in 4-well chamber slides, TYRP1 levels per cell were determined using Volocity software for both transfected and untransfected cells, to account for variations in TYRP1 intensity between wells or slides. The differences between values for transfected and untransfected cells per sample were evaluated using an unpaired T-test, and asterisks indicate statistical significance: *=P<0.05, **=P<0.01, ***=P<0.001. P-values for these samples are ranked in Table 4. Data were collected in a blinded experiment and later annotated with the correct pGIPZ ID. Error bars indicate standard error of the mean.

Figure 4

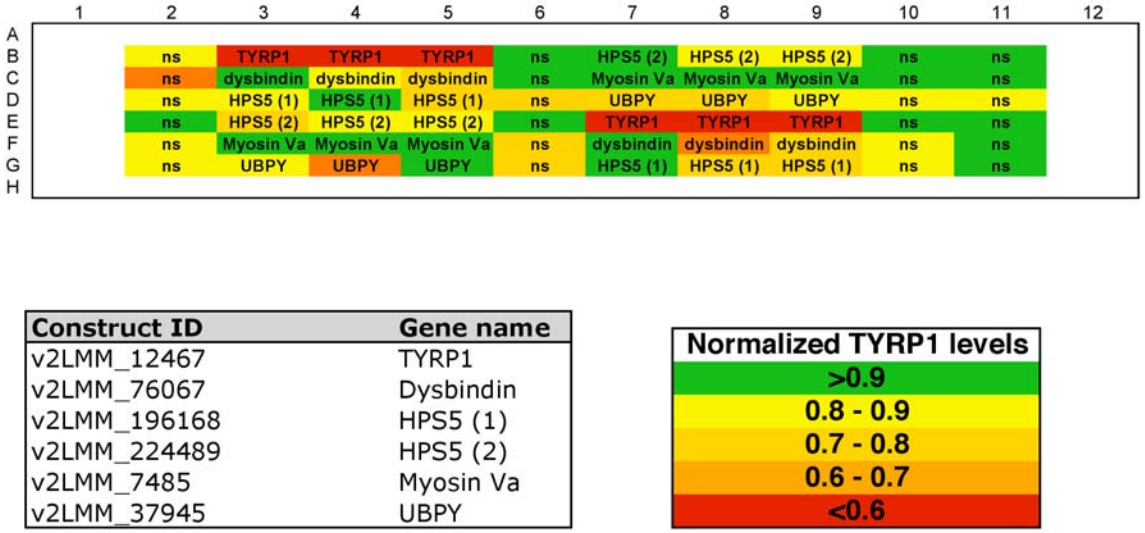

Construct ID	Gene name
v2LMM_12467	TYRP1
v2LMM_76067	Dysbindin
v2LMM_196168	HPS5 (1)
v2LMM_224489	HPS5 (2)
v2LMM_7485	Myosin Va
v2LMM_37945	UBPY

Normalized TYRP1 levels
>0.9
0.8 - 0.9
0.7 - 0.8
0.6 - 0.7
<0.6

Figure 4: Cellomics analysis

The knockdown constructs that led to the highest reduction in TYRP1 levels in melan-a cells on confocal analysis were tested using Cellomics KSR high content analysis. Here TYRP1 levels were measured as the output value SpotTotalIntenPerObjectCh2 of the Spot Detector BioApplication. To correct for variations between wells, the output for transfected cells in every well was normalized to that for untransfected cells in the same well. In this figure, this normalized value is indicated per well by a colour as shown in the legend. Samples are shown in their respective location in a 96-well plate. Only v2LMM_12467 shows a detectable reduction in TYRP1 levels compared to non-silencing controls in Cellomics analysis. See Appendix 2 for data.

Figure 5

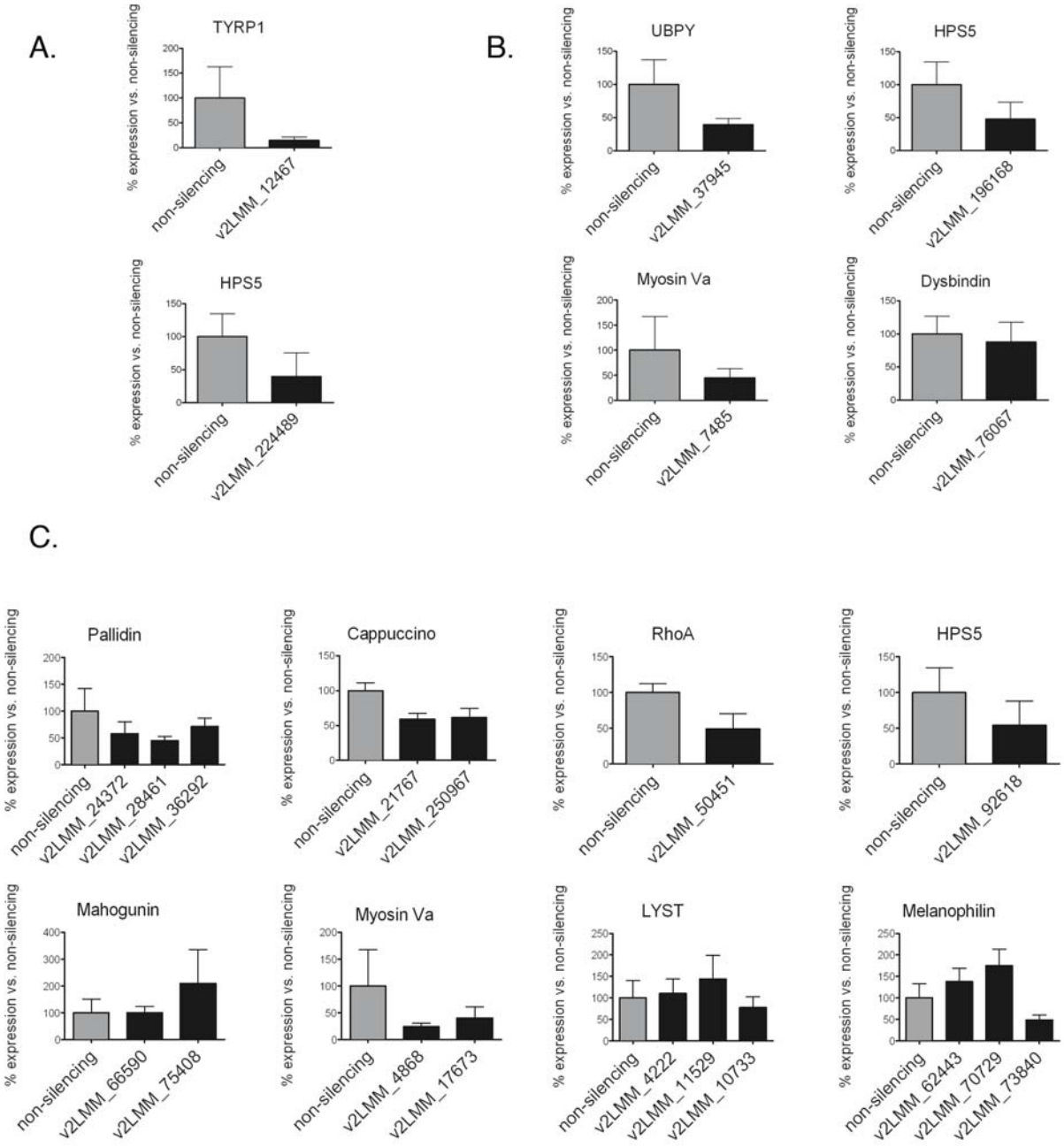

Figure 5: RT-PCR results

RT-PCR results showing residual mRNA levels after knockdown with pGIPZ shRNAmir constructs vs. non-silencing control. All samples were FACS-sorted before RNA isolation, so only cells containing the TurboGFP-expressing pGIPZ vector were analyzed. Error bars indicate standard deviation. **A.** Knockdown efficiency of constructs that showed a reproducible effect on TYRP1 levels in confocal analysis. **B.** Knockdown efficiency of constructs that showed a variable effect on TYRP1 levels in confocal analysis. **C.** Knockdown efficiency of constructs that showed no effect on TYRP1 levels in confocal analysis.

Figure 6

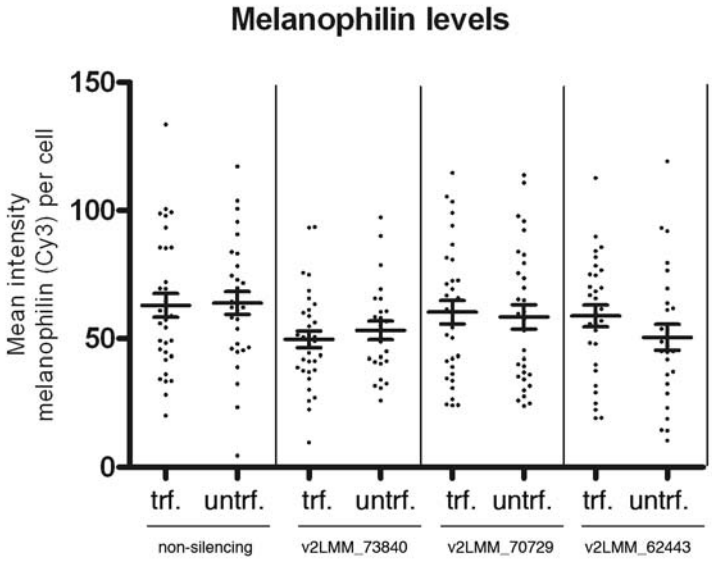

Figure 6: Melanophilin protein levels

Melanophilin levels per cell, quantified using Volocity software from confocal images of cells labeled with an antibody against Melanophilin and secondary Cy3-labeled $F(ab')_2$ antibody fragment. Cells were transfected with pGIPZ constructs transcribing shRNAmir hairpins against melanophilin, or with a non-silencing control. Untransfected cells in each well were measured to account for variation in signal intensities between wells.

Figure 7

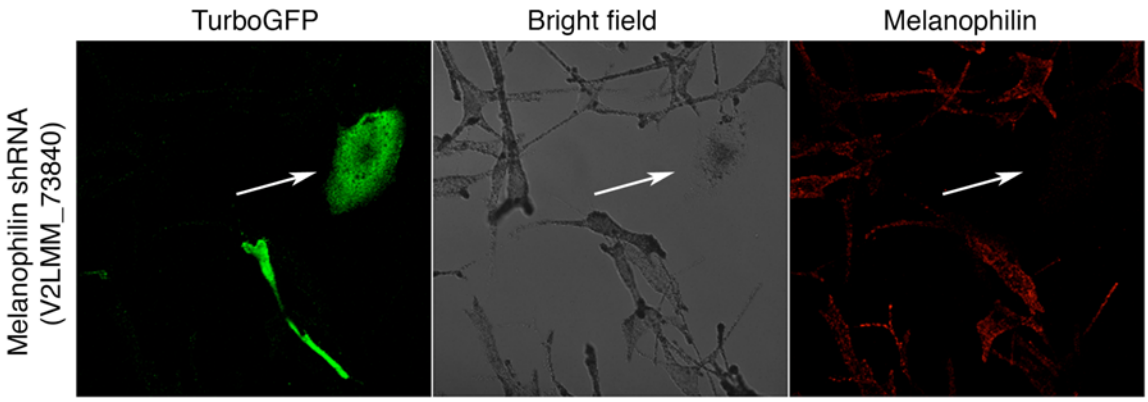

Figure 7: Melanosome transport is inhibited at very low melanophilin levels

In a cell where melanophilin levels are extremely low (last panel, arrow) upon 72 hour knockdown with v2LMM_73840, melanosomes are localized near the nucleus instead of spreading throughout the cell (middle panel).

Appendix 1

Selection parameters and assay setting for Spot Detector BioApplication

These settings of the Spot Detector BioApplication (V2; version 4.1.0.2029) are used to identify melanosomes on Cellomics KSR.

1.1 Selection parameters

Channel 1: Nucleus (Focus channel)		
Object Identification		
Method	IsodataThreshold	
Value	-0.5	
Object Selection Parameter	**Min**	**Max**
ObjectArea	1	500
ObjectShapeBFR	0	1
ObjectShapeBAR	0	10
ObjectAvgInten	0	4095
ObjectTotalInten	0	10000000000
Channel 2: Target		
Object Identification		
Method	FixedThreshold	
Value	25	
Object Selection Parameter	**Min**	**Max**
SpotAreaCh2	0	250000
SpotShapeBFRCh2	0	1
SpotShapeBARCh2	0	10
SpotAvgIntenCh2	25	4095
SpotTotalIntenCh2	0	10000000000
TargetAvgIntenCh2	0	4095
TargetTotalIntenCh2	0	10000000000
Channel 3: GFP		
Object Identification		
Method	None	
Value	1243	
Object Selection Parameter	**Min**	**Max**
SpotAreaCh3	0	33
SpotShapeBFRCh3	0	1
SpotShapeBARCh3	0	1.143
SpotAvgIntenCh3	0	810.485
SpotTotalIntenCh3	0	25746
TargetAvgIntenCh3	25*	4095*
TargetTotalIntenCh3	0	1068080

* These values are for the selection of transfected cells. For the selection of untransfected cells TargetAvgIntenCh3 min=0 and max=24.999

1.2 Assay Settings

Assay Parameters	Value
PixelSize	1.36
MinRefObjectCountPerField	2
SmoothMethodCh1	1
SmoothMethodCh2	1
SmoothMethodCh3	1
SpotCountPerObjectLevelHighCh2	32766
SpotCountPerObjectLevelHighCh2_CC	1
SpotCountPerObjectLevelHighCh3	32766
SpotCountPerObjectLevelHighCh3_CC	1
SpotCountPerObjectLevelLowCh2	0
SpotCountPerObjectLevelLowCh2_CC	1
SpotCountPerObjectLevelLowCh3	0
SpotCountPerObjectLevelLowCh3_CC	1
SpotDetectMethodCh1	1
SpotDetectMethodCh2	2
SpotDetectMethodCh3	1
SpotTotalAreaPerObjectLevelHighCh2	1048576
SpotTotalAreaPerObjectLevelHighCh2_CC	1
SpotTotalAreaPerObjectLevelHighCh3	1048576
SpotTotalAreaPerObjectLevelHighCh3_CC	1
SpotTotalAreaPerObjectLevelLowCh2	0
SpotTotalAreaPerObjectLevelLowCh2_CC	1
SpotTotalAreaPerObjectLevelLowCh3	0
SpotTotalAreaPerObjectLevelLowCh3_CC	1
SpotTotalIntenPerObjectLevelHighCh2	10000000000
SpotTotalIntenPerObjectLevelHighCh2_CC	1
SpotTotalIntenPerObjectLevelHighCh3	10000000000
SpotTotalIntenPerObjectLevelHighCh3_CC	1
SpotTotalIntenPerObjectLevelLowCh2	0
SpotTotalIntenPerObjectLevelLowCh2_CC	1
SpotTotalIntenPerObjectLevelLowCh3	0
SpotTotalIntenPerObjectLevelLowCh3_CC	1
UseMicrometers	0
BackgroundCorrection	50
ObjectSegmentationCh1	5
ResponderDisplayModeCh2	2
ResponderDisplayModeCh3	2
SmoothFactorCh1	1
SmoothFactorCh2	0
SmoothFactorCh3	0
SpotDetectRadiusCh1	0
SpotDetectRadiusCh2	3
SpotDetectRadiusCh3	0
TargetCircModifierCh2	5
TargetCircModifierCh3	0
TargetRingDistanceCh2	0
TargetRingDistanceCh3	0
TargetRingWidthCh2	0
TargetRingWidthCh3	0
UseGatingCh2	1
UseGatingCh3	1
UseReferenceWells	0

Appendix 2

Data from Cellomics analysis used to create Figure 4

Location of samples on plate:

	1	2	3	4	5	6	7	8	9	10	11	12
A												
B		ns	12467	12467	12467	ns	224489	224489	224489	ns	ns	
C		ns	76067	76067	76067	ns	7485	7485	7485	ns	ns	
D		ns	196168	196168	196168	ns	37945	37945	37945	ns	ns	
E		ns	224489	224489	224489	ns	12467	12467	12467	ns	ns	
F		ns	7485	7485	7485	ns	76067	76067	76067	ns	ns	
G		ns	37945	37945	37945	ns	196168	196168	196168	ns	ns	
H												

SpotTotalIntenPerObjectCh2 values for transfected cells (gated by GFP channel: TargetAvgIntenCh3 > 25)

	1	2	3	4	5	6	7	8	9	10	11	12
A												
B		5514.34	3269.08	1900.75	2023.9	3750.3	4579.55	3047.49	2482.83	2946.95	3051.86	
C		4230.45	4252.93	3269.52	3393.15	6908.83	3292.14	7158.78	3347.76	3143.86	2481.87	
D		5368.22	4469.16	7670.35	2957.78	3184.9	2617.88	2062.32	2586.93	2777.26	2332.25	
E		5420.45	3683.38	3211.61	3604.5	4199.65	1953.88	1549.1	1877.64	4646.09	2289.85	
F		4219.2	4303.37	6083.06	3314.59	3199.96	2523.36	2012.44	2416.49	2515.43	1856.39	
G		4799.22	3544.43	2530.83	6961.27	3405.41	3240.78	2178.9	2591.48	2599.84	2473.61	
H												

SpotTotalIntenPerObjectCh2 values for untransfected cells (gated by GFP channel: TargetAvgIntenCh3 < 24.999)

	1	2	3	4	5	6	7	8	9	10	11	12
A												
B		6147.85	5609.09	3870.02	3917.5	4108.33	3111.6	3519.42	2976.54	2892.34	2955.67	
C		6072.38	4639.74	3950.07	4321.65	3997.96	3334.06	2990.84	3006.04	3084.32	2553.95	
D		6545.25	5148.37	4183.15	3873.26	4099.35	3499.58	2598.61	3144.81	3100.21	2691.33	
E		5906.55	5156.12	3978.77	4365.27	3876.45	3366.59	2804.89	3136.73	3068.6	2380.65	
F		5225.82	4558.9	3879.19	3680.21	4145.91	2754.09	3310.67	3152.14	3071.32	1980.98	
G		5860.61	4161.1	3703.07	3122.24	4310.23	3443.5	2931.22	3488.14	3109.96	1497.74	
H												

Normalized value = $[\text{SpotTotalIntenPerObjectCh2}]_{trf}/[\text{ SpotTotalIntenPerObjectCh2}]_{untrf}$

	1	2	3	4	5	6	7	8	9	10	11	12
A												
B		0.8970	0.5828	0.4911	0.5166	0.9129	1.4718	0.8659	0.8341	1.0189	1.0325	
C		0.6967	0.9166	0.8277	0.7852	1.7281	0.9874	2.3936	1.1137	1.0193	0.9718	
D		0.8202	0.8681	1.8336	0.7636	0.7769	0.7481	0.7936	0.8226	0.8958	0.8666	
E		0.9177	0.7144	0.8072	0.8257	1.0834	0.5804	0.5523	0.5986	1.5141	0.9619	
F		0.8074	0.9439	1.5681	0.9007	0.7718	0.9162	0.6079	0.7666	0.8190	0.9371	
G		0.8189	0.8518	0.6834	2.2296	0.7901	0.9411	0.7433	0.7429	0.8360	1.6516	
H												